



## Qualitative Temperature Variation Imaging by Thermoreflectance and SThM Techniques

Stéphane Grauby, A. Salhi, L.D. Patino Lopez, S. Dilhaire, B. Charlot, W.  
Claeys, B. Cretin, G. Tessier, N. Trannoy, P. Vairac, et al.

### ► To cite this version:

Stéphane Grauby, A. Salhi, L.D. Patino Lopez, S. Dilhaire, B. Charlot, et al.. Qualitative Temperature Variation Imaging by Thermoreflectance and SThM Techniques. THERMINIC 2005, Sep 2005, Belgirate, Lago Maggiore, Italy. pp.284-289. hal-00189487

**HAL Id: hal-00189487**

**<https://hal.science/hal-00189487>**

Submitted on 21 Nov 2007

**HAL** is a multi-disciplinary open access archive for the deposit and dissemination of scientific research documents, whether they are published or not. The documents may come from teaching and research institutions in France or abroad, or from public or private research centers.

L'archive ouverte pluridisciplinaire **HAL**, est destinée au dépôt et à la diffusion de documents scientifiques de niveau recherche, publiés ou non, émanant des établissements d'enseignement et de recherche français ou étrangers, des laboratoires publics ou privés.

# Qualitative Temperature Variation Imaging by Thermoreflectance and SThM Techniques

*S. Grauby<sup>1</sup>, A. Salhi<sup>1</sup>, L-D. Patino Lopez<sup>1</sup>, S. Dilhaire<sup>1</sup>, B. Charlot<sup>2</sup>, W. Claeys<sup>1</sup>  
B. Cretin<sup>3</sup>, S. Gomes<sup>3</sup>, G. Tessier<sup>3</sup>, N. Trannoy<sup>3</sup>, P. Vairac<sup>3</sup> and S. Volz<sup>3</sup>*

<sup>1</sup>Centre de Physique Moléculaire Optique et Hertzienne, Université Bordeaux 1, 351, cours de la Libération, 33405 Talence cedex, France,

<sup>2</sup>TIMA, 46 avenue Félix Viallet, 38031 Grenoble, France,

<sup>3</sup>Groupement de Recherche Micro et Nanothermique, GDR CNRS 2503, Ecole Centrale Paris, Grande Voie des Vignes, 92295 Châtenay Malabry, France.

[s.grauby@cpmoh.u-bordeaux1.fr](mailto:s.grauby@cpmoh.u-bordeaux1.fr)

## ABSTRACT

We have studied temperature variations on two dissipative structures with two different techniques. The dissipative structures are constituted of thin ( $0.35\mu\text{m}$ ) dissipative resistors, the distance between two resistors being equal to  $0.8$  or  $10\mu\text{m}$ . On one hand, we have used a thermoreflectance imaging technique which is a well-known non contact optical method to evaluate temperature variations but whose spatial resolution is limited by diffraction. On the other hand, we have used a Scanning Thermal Microscope (SThM) to study the thermal behaviour of these small dissipative structures. We compare qualitative results obtained by both methods and we present their advantages and limitations for temperature measurements on microelectronic devices.

## 1. INTRODUCTION

As integration density of microelectronic circuits goes increasing, there is a need for methods able to measure local temperature variations at submicronic scales.

As a consequence, well-known methods such as infrared imaging [1], liquid crystals or thermocouple measurements [2] are not adapted to this kind of samples as they offer a bad spatial resolution ( $5$  to  $10\mu\text{m}$  minimum) regarding the device dimensions. Moreover, a thermocouple implies a contact with the sample that can damage it or disrupt its functioning.

Among the optical methods for submicronic thermal mapping, thermoreflectance[3-5] is a useful non contact and non invasive method which presents a good spatial resolution as limited by diffraction to the order of magnitude of the illuminating wavelength.

Nevertheless, when studying structures as thin as a few hundreds nanometers, Scanning Thermal Microscope (SThM) seems the only technique able to reach temperature variation measurements at this scale.

In this paper, we have used the last two methods to qualitatively study the temperature variations on the same samples and we propose to compare their performances.

## 2. SAMPLE UNDER TEST

We have studied two kinds of structures constituted by a series of 9 parallel strips resistors which serve themselves as a heat source. Indeed, supplying them with a current, they are submitted to a variation of temperature. The width of each resistor is  $0.35\mu\text{m}$ . They are covered by a passivation layer made of silicon oxide. The difference between both structures is the spacing between the resistors. In the first one (figure 1), the distance between two consecutive resistors is  $10\mu\text{m}$  whereas it is only  $0.8\mu\text{m}$  in the second one (figure 2). These structures are part of a whole test device designed for the evaluation of various temperature measurement techniques; the first one is named C5 while the second one is named C3. The die was implemented using  $0.35\mu\text{m}$  CMOS technology.

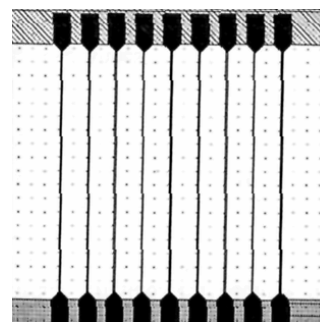


Figure 1: Sample 1 (C5) constituted of nine  $0.35\mu\text{m}$  thin resistors (distance between 2 resistors:  $10\mu\text{m}$ )

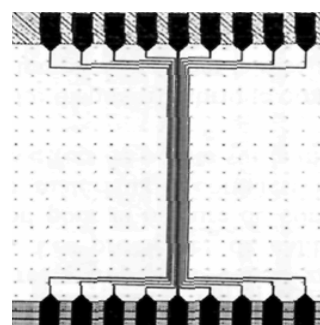


Figure 2: Sample 2 (C3) constituted of nine  $0.35\mu\text{m}$  thin resistors (distance between 2 resistors:  $0.8\mu\text{m}$ )

### 3. THERMOREFLECTANCE MEASUREMENTS

Reflected light coming from the surface of a sample carries information about the thermomechanical behavior of the device under test via parameters such as amplitude, phase, polarization etc... of light. Thermoreflectance is a useful non contact technique to measure temperature variations of a device submitted to a current.

Indeed, when an electrical current supplies an electronic device, the latter is submitted to a temperature variation  $\Delta T$ , which creates a reflectivity variation  $\Delta R$  at the device surface:

$$\frac{\Delta R}{R} = \frac{1}{R} \frac{\partial R}{\partial T} \Delta T = \kappa \Delta T \quad (1)$$

where  $R$  is the sample mean reflectivity and  $\kappa$  is the thermoreflectance coefficient depending on the nature of the material, on the passivation layer thickness[6], on the light wavelength[7-8]... The reflectivity variation implies an intensity variation of the light reflected to the photodetector (CCD camera, photodiode). Thus, measuring the relative variation of photocurrent  $\Delta I/I$  of the detector, we can deduce the relative variation of reflectivity  $\Delta R/R$  and then the temperature variation  $\Delta T$  of the sample if  $\kappa$  is known. Unfortunately, the value of  $\kappa$  is often only known for a few bulk materials at a precise wavelength under specific experimental conditions. Besides, in microelectronic devices, the structure, in particular the passivation layer thickness, has a great influence on this coefficient value and we cannot use the bulk material value. As a consequence, every studied sample and every experimental set-up need a new calibration. Once the value of this coefficient is determined, you can obtain absolute temperature variations.

The set-up is presented in figure 3. The luminous source is LED whose intensity can be modulated. The lenses ( $L_1$ ) and ( $L_2$ ) enable to adapt the size of the luminous beam to the size of the object under study. As we use a polarizing beam splitter (PBS) and as the light emitted by the LED is not polarized, a sheet polarizer ( $P_1$ ) is used to polarize it and to adjust the light intensity to send upon the device under test. After reflection on the sample and crossing twice the quarter-wave plates ( $P_2$ ), the polarisation has been exchanged. As a consequence, the beam is being transmitted in the detection arm ended by a CCD camera. In this arm, the lens ( $L_3$ ) enables to image the sample onto the CCD detector. Its video frequency is fixed and equal to 50Hz. The output signal of the camera is analyzed by a computer to extract the information. All elements  $L_1$ ,  $L_2$ ,  $P_1$ ,  $P_2$  and PBS are included in a microscope.

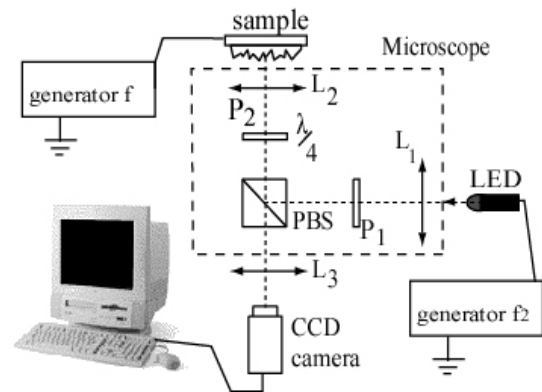


Figure 3: Modulated thermoreflectance set-up

The sample is submitted to a sinusoidal current at frequency  $f$  and the flux of the LED is also modulated. Indeed, we use an heterodyne thermoreflectance imaging system[9]. The heating, due to Joule effect, occurs at  $f_1$  (equal to  $2f$  or  $f$  depending on the electrical excitation waveform) and the LED flux is modulated at  $f_2 = f_1 + 12.5\text{Hz}$ . The phenomenon of interest, i.e. the heating of the device initially at  $f_1$ , can then be observed at the blinking frequency  $f_2 - f_1 = 12.5\text{Hz}$  which is easily analyzed by the camera which works at 50Hz. Therefore, during a period of the signal of interest, we take 4 images and we use a classical 4 images algorithm[10] to deduce the relative reflectivity variation amplitude  $\Delta R/R$  and phase  $\phi$ . Moreover, we accumulate several hundreds or thousand images to improve the signal to noise ratio which depends on the square root of the number of accumulated images.

### 4. SCANNING THERMAL MICROSCOPY

Thus, scanning thermal microscopy is a promising method that could enable to detect temperature variations on very small structures at submicrometric scale, and in particular here on each resistor individually. Indeed, a SThM can measure the amplitude (and the phase) of the temperature variations induced by the AC current along the electrically excited sample. The SThM is a conventional atomic force microscope (AFM) mounted with a specific probe. The AFM system enables the control of the tip position and the contact force with the sample (Figure 4). Monitoring is performed with a feedback loop between the signal of three x-y-z piezo-electrical ceramics carrying the tip cantilever and four photodiodes tracking a laser beam which is reflected on the mirror of the probe.

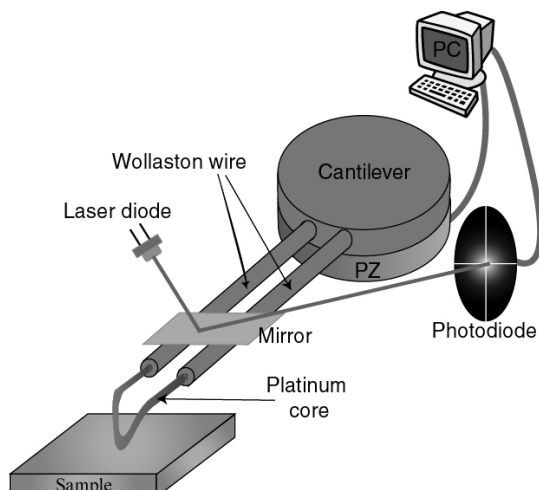


Figure 4: STHM schematic view

This probe is constituted of a Wollaston wire shaped into a tip and etched to uncover its core platinum (Pt). The Pt wire is included in a Wheatstone bridge and used as a thermistor, as the resistance of the wire depends on its temperature. The STHM is used in an AC regime. As a consequence, we use a lock-in scheme to measure the amplitude (and the phase) of the first harmonic in the tip voltage. From these measurements, we deduce the amplitude (and the phase) of the temperature at the surface of the sample. The bridge voltage is measured while scanning the surface so that the Pt electrical resistance could be estimated at each point of the sample surface. We estimate the diameter of the tip to be of the order of 5  $\mu\text{m}$  and its contact radius of the order of 50 nm. Therefore, spatial resolution better than the one reached with thermoreflectance techniques can be expected[11].

We have already used this technique in AC regime[12] and we have in particular measured quantitative temperature variations on PN  $\text{Bi}_2\text{Te}_3$  thermoelectric couples[13].

## 5. THERMOREFLECTANCE RESULTS

We have first used the set-up described in paragraph 3 on the C5 device with  $f_1=300$  Hz and  $f_2=312,5$  Hz. The current supplying the resistors is a few mA, the resistor of C3 or C5 being equal to a few hundreds ohms. The lens  $L_2$  used is a  $\times 50$  microscope objective and the LED is a red one emitting at 660 nm. The image of reflectivity, showing a zoom of the central part of C5, is presented in figure 5. Every image we present in this section is the result of accumulation of 40000 images corresponding to an acquisition time of about ten minutes. We clearly see the reflectivity variation to be maximal on the heating resistors (4 resistors in this image).

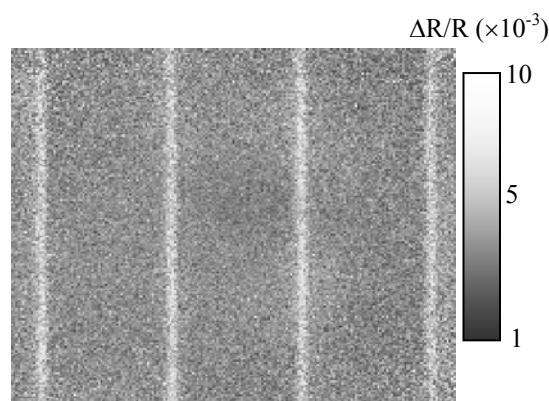


Figure 5: Relative reflectivity variation amplitude on C5 device.

Then, we have used this set-up to measure reflectivity variations on the C3 device in the same experimental conditions. The  $\Delta R/R$  amplitude image is presented in figure 6. As expected, we can note a higher variation of reflectivity in the heating zone but we do not distinguish the different resistors. This clearly shows that the spatial resolution is too limited.

The use of a LED is then all the more adapted as we can easily find LEDs emitting at various wavelength. As the spatial resolution is limited by diffraction and then linked to the illumination wavelength, it seems logical to use a blue LED ( $\lambda=450\text{nm}$ ). The other experimental conditions being unchanged, the  $\Delta R/R$  image is presented in figure 7. And here we can individually distinguish the 9 thin resistors. Nevertheless, it is obvious that we reach the resolution limit.

But we can use a  $\times 100$  microscope objective to improve the quality of the image. The result is presented in figure 8 where the 9 resistors are more distinguishable.

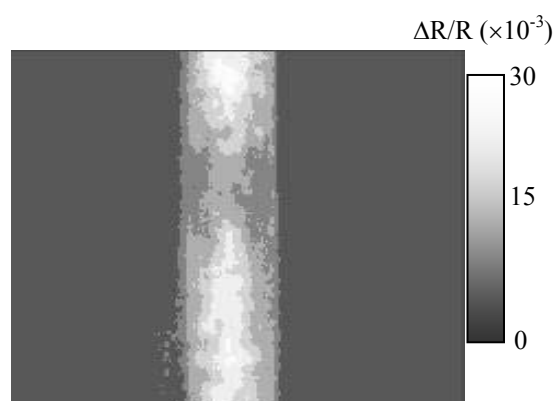


Figure 6: Relative reflectivity variation amplitude on C3 device with red led.

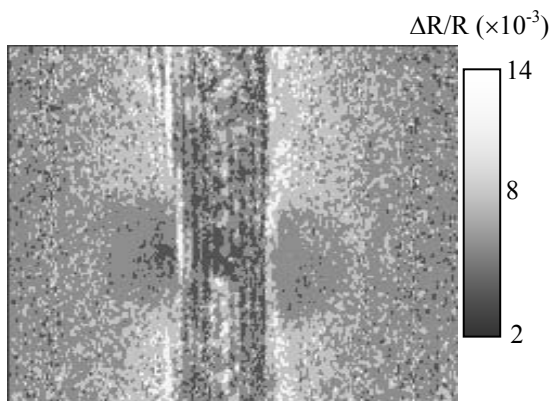


Figure 7: Relative reflectivity variation amplitude on C3 device with blue led.

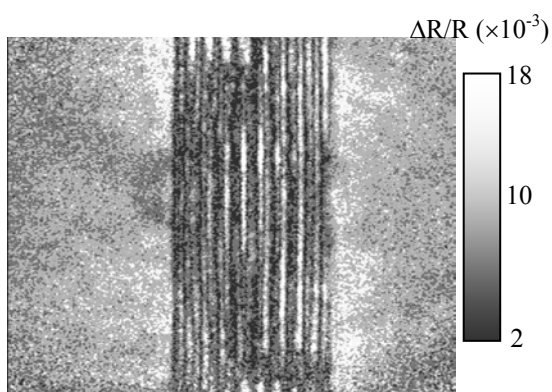


Figure 8: Relative reflectivity variation amplitude on C3 device with blue led and  $\times 100$  microscope objective.

So, these experiments show that thermoreflectance can be a powerful technique to study the thermal behaviour of highly integrated microelectronic devices. In particular, the use of a LED as light source is very interesting as we can easily change the illumination wavelength to improve the spatial resolution. Indeed, if working with a microscope objective under high magnification conditions ( $\times 50$  or  $100$ ) and with high numerical aperture, we have obtained thermoreflectance images of  $0.35\ \mu\text{m}$  structures.

There is still remaining the issue of calibration. There are different materials constituting the device and each needs a calibration of its thermoreflectance coefficient. There exist various methods[2, 8, 14] but none is universal and each method must be adapted to the experimental configuration, the calibration sometimes proving quite difficult. Moreover, the signal to noise ratio is not very good and needs to be improved. One solution is to accumulate more images. But then, it takes a lot of time and point thermoreflectance measurements with a photodiode and a lock-in amplifier becomes then a better method. We are now working on another technique combining point measurements with imaging techniques.

## 6. STHM RESULTS

We have then used the set-up described in paragraph 4 to study the structures C3 and C5. Here, the device is supplied by a sinusoidal current and the heating occurs at  $f_1$ . A lock-in scheme measures the tip voltage amplitude (and phase) at frequency  $f_1$ . We can adjust the scan size, the scan rate (speed of the tip) and the number of samples by line. We choose the frequency  $f_1$  so that the lock-in time constant should be compatible with the tip scan rate.

We first studied C5 with  $f_1$  equal to 1 kHz, the current supplying C5 is a few mA, the scan size is  $30\mu\text{m}\times 30\mu\text{m}$ , the scan rate 0.2 Hz and a line is constituted of 256 samples. We clearly see (figure 9) 3 resistors heating. The amplitude is in arbitrary units. The spacing between two resistors corresponds to the expected  $10\ \mu\text{m}$ . The thermal signal spread over about  $1\ \mu\text{m}$  on each resistor. The tip sweeps the device surface hence the passivation layer and not directly the resistors. So, the temperature signal due to the heating resistors is “filtered” and then smoothed by the passivation layer. The image consequently corresponds to a qualitative surface temperature mapping and not of the active zone.

We have then supplied C3, all the parameters are the same as for C5 apart for the scan size which is first reduced to  $15\ \mu\text{m}\times 15\ \mu\text{m}$ . We clearly detect (figure 10) the heating zone constituted by the 9 resistors but we do not see them individually.

Hence, we have once again reduced the scan size to  $4\ \mu\text{m}$  and registered the signal on a section of the resistors (figure 11). We detect 3 maxima perhaps corresponding to 3 heating resistors but the signal to noise ratio is poor and other experiments need to confirm these results. The spacing between 2 maxima is a little more than  $1\ \mu\text{m}$  which is compatible with the  $0.8\ \mu\text{m}$  spacing given by the constructor taking into account the result obtained on C5 showing that, under the same conditions, the thermal signal spreads over about  $1\ \mu\text{m}$  on each resistor, thus reaching the neighboring resistor on C3.

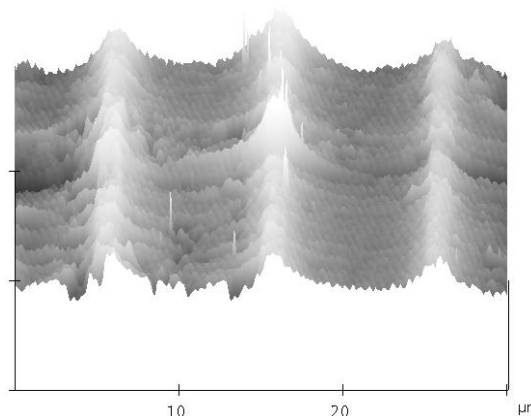


Figure 9: Qualitative SThM temperature image of the C5 device surface.

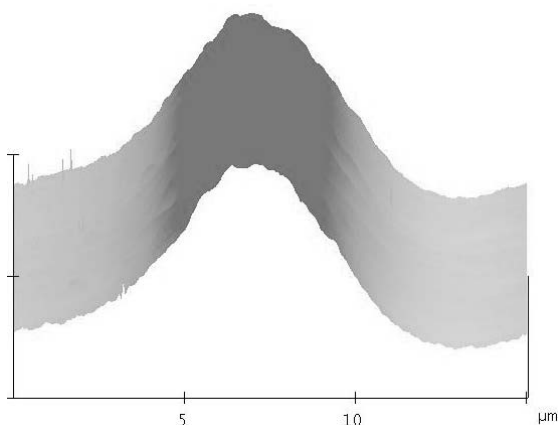


Figure 10: Qualitative SThM temperature image of the C3 device surface.

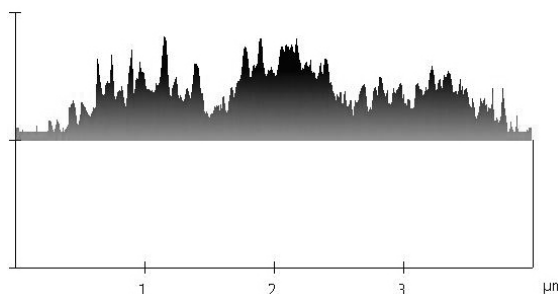


Figure 11: Qualitative SThM temperature on a section of the C3 device surface.

The method presents several drawbacks. First of all, if we want to measure microelectronic device temperature, the passivation layer needs to be eliminated to access the active zone or a model must be developed to take it into account but it implies that the passivation layer structure must be perfectly known for every point of the sample.

Moreover, it is time consuming as the whole image (figure 9 or 10 for instance) needs about 20 mn. If we want to reduce it, it is necessary to increase the scan rate and then to reduce the lock-in time constant hence to increase  $f_1$ . But then the thermal signal amplitude decreases and the signal to noise ratio also decreases. This decrease adds to the one due to the passivation layer. Besides, because of the dimension of the Pt core hiding the much smaller contact tip, it is not easy to precisely localize the scanned area before seeing the resulting image, in particular when the scan size is small.

Finally, the tip temperature is not the sample temperature. We have developed [13] a model taking into account the tip-sample heat transfer. We plan to use it to deduce the sample surface temperature.

## 7. CONCLUSION

We have evaluated two thermal measurement methods in terms of spatial resolution and calibration issue. We have used a very integrated microelectronic device and shown that thermorefectance can be efficient if using an appropriate optical system. The spatial resolution can then be very good but the main issue is the calibration and the signal to noise ratio. We are now developing a method to improve it while maintaining a small acquisition time; it will constitute a compromise between point and imaging techniques.

As for SThM, again, the passivation layer is an issue as the tip measures the temperature on its surface and not on the active zone itself. It is consequently not obvious to measure the active zone temperature. Moreover, submicrometric spatial resolution for thermal mode is not clearly proved.

## 8. ACKNOWLEDGEMENT

The samples have been provided by the GDR Micro et Nanothermique (n°G2503).

This work has been supported by the Conseil Régional d'Aquitaine and by a FEDER fellowship.

## 9. REFERENCES

- [1] M. Grecki, J. Pacholik, B. Wiecek and A. Napieralski, "Application of computer-based thermography to thermal measurements of integrated circuits and power devices", *Microelectronics Journal*, vol. 28, pp. 337-347, 1997.
- [2] G. Tessier, S. Holé and D. Fournier, "Quantitative thermal imaging by synchronous thermorefectance with optimized illumination wavelengths", *Applied Physics Letters*, vol. 78, pp. 2267-2269, 2001.
- [3] S. Dilhaire, S. Grauby, S. Jorez, L-D Patino Lopez, E. Schaub and W. Claeys, "Laser diode COFD analysis by thermorefectance microscopy", *Microelectronics Reliability*, vol. 41, pp. 1597-1601, 2001.
- [4] J.-P. Bardon, E. Beyne, J.-B. Saulnier, *Thermal Management of Electronic Systems III-Eurotherm 58*, (Elsevier Health Sciences, Paris, 1998).
- [5] J. Opsal, A. Rosencwaig and D. L. Wilenborg, "Thermal-wave detection and thin-film thickness measurements with laser beam deflection", *Applied Optics*, vol. 22, pp. 3169-76, 1983.
- [6] V. Quintard, G. Deboy, S. Dilhaire, D. Lewis, T. Phan, and W. Claeys, "Laser beam thermography of circuits in the particular case of passivated semiconductors", *Microelectronic Engineering*, vol. 31, pp. 291-298, 1996.
- [7] J. Heller, J. W. Bartha, C. C. Poon and A. C. Tam, "Temperature dependence of the reflectivity of silicon with surface oxide at wavelengths of 633 and 1047 nm", *Applied Physics Letters*, vol. 75, n°1, pp. 43-45, 1999.

- [8] S. Grauby, G. Tessier, S. Holé and D. Fournier, "Quantitative thermal imaging with CCD array coupled to an heterodyne multichannel lock-in detection", *Analytical Science*, vol. 17, pp. 67-69, 2001.
- [9] S. Grauby, B.C. Forget, S. Holé and D. Fournier, "High resolution photothermal imaging of high frequency phenomena using a visible CCD camera associated with a multichannel lock-in scheme", *Review of Scientific Instruments*, vol. 70, pp. 3603-3608, 1999.
- [10] P. Gleyzes, F. Guernet et A. C. Boccara, "Profilométrie picométrique. II. L'approche multi-détecteur et la détection synchrone multiplexée", *Journal of Optics (Paris)*, vol. 26, n°6, pp. 251-265, 1995.
- [11] S. Gomes and D. Ziane, "Investigation of the electrical degradation of a metal-oxide-silicon capacitor by scanning thermal microscopy", *Solid-State-Electronics*, vol. 47, pp. 919-22, 2003.
- [12] Y. Ezzahri, L. D. Patiño Lopez, O. Chapuis, S. Dilhaire, S. Grauby, W. Claeys and S. Volz, "Dynamical Behavior of the Scanning Thermal Microscope (SThM) Thermal Resistive Probe using Si/SiGe Microcoolers", *Superlattices and Microstructures*, accepted for publication, april 2005.
- [13] L-D. Patiño-Lopez, S. Grauby, S. Dilhaire, M-A. Salhi, W. Claeys, S. Lefèvre, S. Volz, "Characterization of the thermal behaviour of PN thermoelectric couples by scanning thermal microscope", *Microelectronics Journal*, vol. 35, pp. 797-803, 2004.
- [14] S. Dilhaire, S. Grauby and W. Claeys, "Calibration procedure for temperature measurements by thermoreflectance under high magnification conditions", *Applied Physics Letters*, vol. 84, pp. 822-824, 2004.